Proceedings of the Second International Conference on Press-in Engineering 2021, Kochi, Japan – Matsumoto et al (eds)

Study on a countermeasure method for liquefaction of fishing ports against the Nankai Trough Earthquake

K. Okabayashi, G. Hashimura, A. Okubo, H. Ogasawara & S. Kadowaki
Kochi National College of Technology, Nankoku city, Kochi, Japan

K. Tokuhisa
Chodai Co., Ltd, Chuo Ward, Tokyo, Japan

ABSTRACT: In the near future, the Nankai Trough earthquake is expected to occur in Japan. It may be difficult to receive the prompt rescue and support in the event of this disaster since the Kochi Prefecture is surrounded by steep mountains. Therefore, Kochi Prefecture has placed earthquakeproof berths, but we propose that fishing ports also be used as disaster prevention bases. In this study, we investigated the liquefaction countermeasures for fishing port quays using sheet piles. As a result, (1) It was found out that the construction method using sheet piles was not enough for liquefaction countermeasures. (2) The method using sandbags and permeable steel sheet piles confirmed the effect of suppressing liquefaction.

1 INTRODUCTION

The 2011 off the Pacific coast of Tohoku Earthquake on March 11, 2011 is the largest earthquake in the observation history of Japan, caused huge damage by tsunami and liquefaction. All the ports on the Pacific side from Hachinohe Port in Aomori Prefecture to Kashima Port in Ibaraki Prefecture were damaged. Several damages such as settlements of structure and large faulting between the quays were seen in the damaged ports. But fishing ports and harbors contributed greatly to recovery after the earthquake because the port function was quickly restored.

The probability of the Nankai Trough Earthquake to occur within the next 30 years is estimated to be between seventy and eighty percent. When the Nankai Trough Earthquake occurs, there is a risk of damage to a wide area from Kyushu region to Tokai region. After the earthquake, Kochi Prefecture may have difficulty receiving help such as transportation of supplies from the land route as it is surrounded by steep mountains.

There are 88 fishing ports in Kochi Prefecture, it is considered that some of the fishing ports will be used as disaster prevention centers at the time of the earthquake, as in the case of the Tohoku Region Pacific Ocean Earthquake. Currently, seismic reinforcement and maintenance of several fishing ports, which are disaster prevention bases, are in progress.

In this study, we investigated an earthquakeproof berth focusing on the drainage near the quay wall.

From the previous study (Kiwa 2016), the following can be seen about the quay wall using the double steel sheet pile method at the time of the earthquake. (1) The quay using the double steel sheet pile method was able to suppress the deformation compared to the untreated quay. However, it was not possible to keep the allowable values for deformation and settlement of the quay wall. (2) There was a phenomenon that the excess pore water pressure ratio increases near the wall of the quay compared to the untreated quay. It is necessary to dissipate the excess pore pressure in the vicinity of the quay wall to prevent liquefaction. Therefore, the purpose of this study is to reduce displacement and reduce excess pore water pressure near the quay wall.

For the research method, the liquefaction analysis by effective stress analysis method (SoilWorks for LIQCA) and the liquefaction experiment by dynamic centrifuge model test were used. We examined the behavior of the quay during an earthquake from the analysis results and the experimental results.

2 RESEARCH CASE

In this study, we examined the four models. No countermeasure (Figure 1), a double steel sheet piling (Figure 2), a combination of double steel sheet piling with sandbags (Figure 3), a double steel sheet piling method of permeable steel sheet piling with sandbags (Figure 4). We call them Case1, Case2, Case3, and Case4 respectively. The

DOI: 10.1201/9781003215226-43

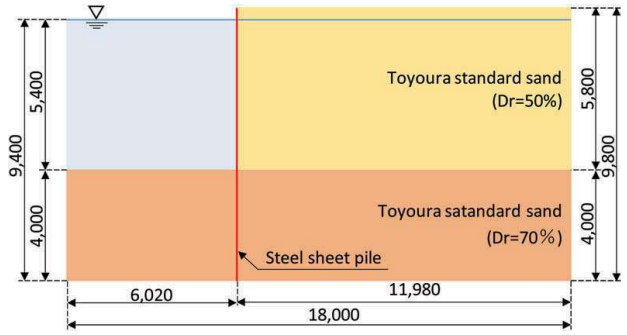

Figure 1. Case1.

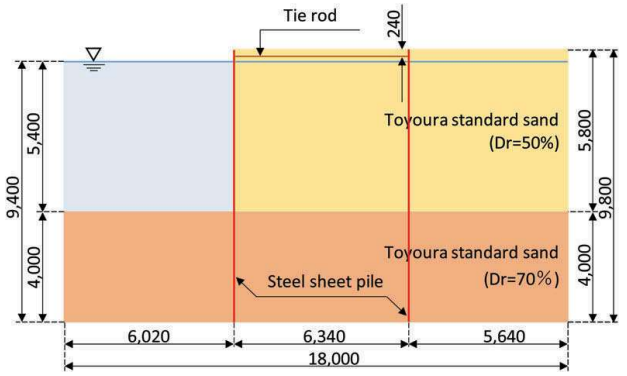

Figure 2. Case2.

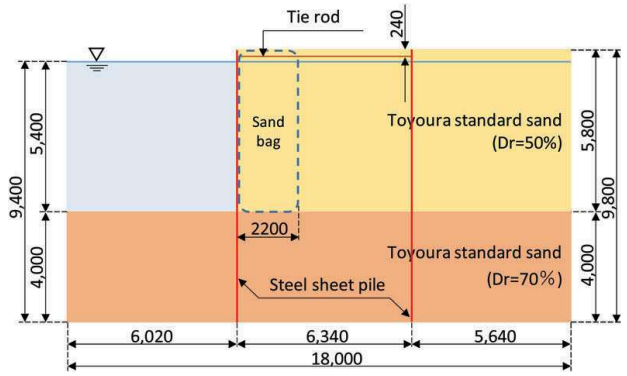

Figure 3. Case3.

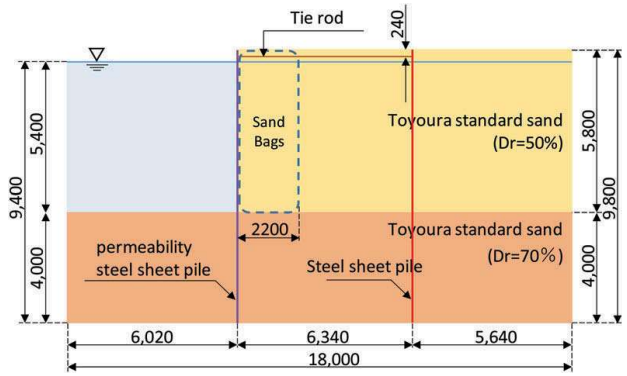

Figure 4. Case4.

Case4 is a model that uses a permeable steel sheet pile for the quay wall of Case3. The Toyoura sand with Dr = 70% is used for the base layer, and that with Dr = 50% is used for the liquefaction layer.

The sandbags used in Case3 and Case4 are made by putting light gravel material (pearl white: γ_t = 16.02kN/m^2) in a high permeability bag (non-woven). In the analysis, the integration effect of sandbags is not considered, and it is regarded as an additional effect. Japanese Association for Steel Pipe Piles (2017) proposed permeable steel sheet piles. The steel sheet piles have almost natural water circulation and water permeability by providing small holes for water permeability in the steel sheet piles. A permeability hole is placed in the soil layer portion. The installation location is necessary to consider the future dredging depth, scouring depth, the occurrence of piping, etc.

Regarding the arrangement of permeable holes, we referred to Table 1 Example of the arrangement of permeability holes. In this study, the hole diameter at the effective width of 500 mm was adopted, and the number of holes per unit depth was set to 5.

3 LIQUEFACTION ANALYSIS

3.1 *Analysis method*

As an analysis method, the liquefaction analysis is performed using SoilWorks for LIQCA. LIQCA (LIQCA Liquefaction Geo-Research Institute 2015) is a liquefaction analysis program based on effective stress, using the u-p formulation with the solid-phase displacement (u) and the pore water pressure (p) as unknowns. Figure 5 shows the analysis procedure.

Table 1. Example of water hole arrangement.

Effective width (mm)	Hole diameter D (mm)	Hole spacing L(mm)	Rate hole ratio
900	80	1000	0.56
600	65	1000	0.55
500	60	1000	0.57

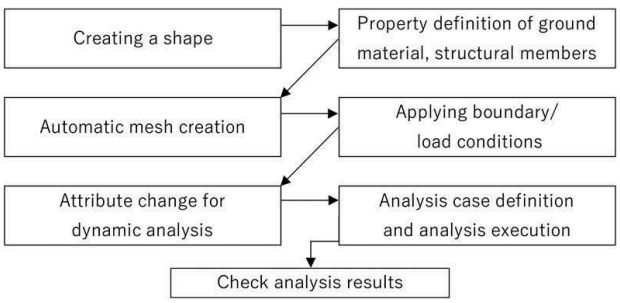

Figure 5. Analysis procedure.

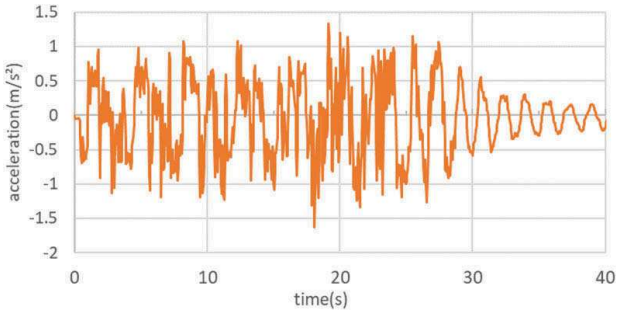

Figure 6. Input seismic wave.

3.2 *Input seismic wave*

The magnitude of the required acceleration was calculated and set based on the simple judgment method in the Specification for Highway Bridges (Japan Road Association 2012). Figure 6 shows the seismic waves used for the analysis. The maximum acceleration is 168.2gal.

3.3 *Analysis model*

In this study, we analyzed two models, a model based on actual ground (hereinafter, it is called a real model) and a model for liquefaction experiment (hereinafter, it is called an experimental model). In the actual model, the actual fishing port quay was modeled, the analysis area was enlarged, and the side surface was a repeating boundary and the bottom surface was a viscous boundary. The main purpose was to see the effect of the analysis area on the analysis results.The experimental model is used for comparison with the liquefaction experiment.

In SoilWorks for LIQCA2D15(2015), it is necessary to set boundary conditions for soil skeleton and pore water. We defined all boundary and load conditions used for both static and dynamic analyses. Figures 7 and 8 show the boundary conditions of the experimental model, Figures 9 and 10 show the boundary conditions of the real model. In the real model, the width of the analysis model is increased in consideration of the propagation of seismic waves.

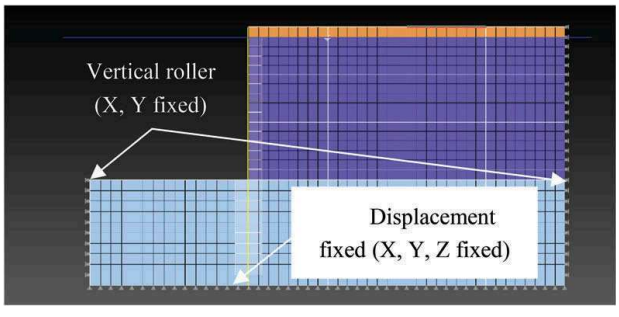

Figure 7. Side and bottom boundary conditions (Experimental model).

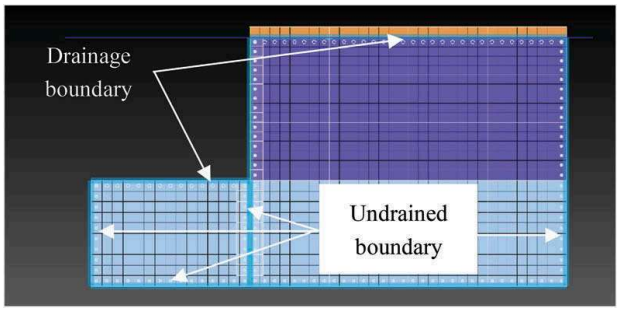

Figure 8. Drainage boundary condition (Experimental model).

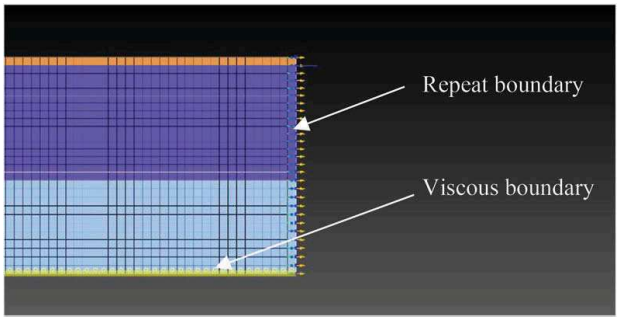

Figure 9. Side and bottom boundaries (Real model).

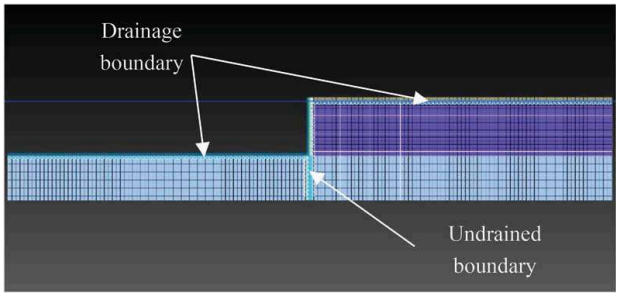

Figure 10. Drainage boundary condition (Real model).

3.4 *Materials parameter*

Tables 2 and 3 show the physical properties of the ground materials, Table 4 shows the physical properties of the materials used for countermeasures, and Table 5 shows the analysis condition. In this study, ground material properties were set with reference to the parameters used by Saito (2016).

The parameter of Toyoura sand (Dr = 50%) used for the liquefaction layer was determined by performing the element simulations in SoilWorks for LIQCA (2015) to match the results of the box shear test (Tanimoto, 2019) conducted at our university as shown in Figure 11. The physical properties of the steel sheet piles and the permeable steel sheet piles were determined based on the references (NIPPON STEEL CORPORATION 2019), respectively.

Table 2. Parameters for static analysis.

Item	Unit	Toyoura sand (Dr=50%)		Toyoura sand (Dr=70%)	Sand bags	
		Above water	Under water		Above water	Under water
Wet unit volume weight(γt)	kN/m^3	14.48	14.48	15.06	17.08	17.08
Satureted unit volume weight(γ_{sat})	kN/m^3	18.77	18.77	18.80	19.26	19.26
Element depth	m	1.0	1.0	1.0	1.0	1.0
Poisson's ratio		0.333	0.333	0.333	0.333	0.333
Effective soil covering pressure	kN/m^2	1.0E-08	1.0E-08	1.0E-08	1.0E-08	1.0E-08
Ststic earth pressure coefficient		1.0	1.0	1.0	1.0	1.0
Propertionality coefficient of Young's modules (E_0)		2775.2	2775.2	2775.2	5098.4	5098.4
Constant(n)		1.0	1.0	1.0	1.0	1.0
Adhesive force	kN/m^2	0.0	0.0	0.0	0.0	0.0
Internal friction angle (φ)		37.75	37.75	37.75	37	37

Table 3. Parameter for dynamic analysis.

Item	Unit	Toyoura sand (Dr=50%)		Toyoura sand (Dr=70%)	Sand bags	
		Above water	Under water		Above water	Under water
Wet unit volume weight(γt)	kN/m^3	14.48	14.48	15.06	17.08	17.08
Satureted unit volume weight(γ_{sat})	kN/m^3	18.77	18.77	18.80	19.26	19.26
Element depth	m	1.0	1.0	1.0	1.0	1.0
Poisson's ratio		0.0	0.0	0.0	15.5	15.5
Static earth pressure coefficient		0.0	0.0	0.0	0.5	0.5
Nondimensional initial shear coefficient		910	910	1040.9	761	761
Initial gap ratio (e_0)		0.791	0.791	0.718	0.8	0.8
Compression exponent (λ)		0.0039	0.0039	0.0039	0.025	0.025
Sweling index (K)		0.00022	0.00022	0.00022	0.0003	0.0003
Pseude-consideration ratio		1.0	1.0	1.5	1.0	1.0
Dilatancy factor (D_0)		0.0	0.5	0.75	0.0	1.0
Dilatancy factor (n)		0.0	5.0	7.0	0.0	4.0
Water permeability/ Unit volume of water	m/sec/kN/m^3	0.0	0.0001	0.0001	0.0	0.00022
Bulk elastic modules of water	kN/m^2	2000000	2000000	2000000	2200000	2200000
S wave velocity	m/sec	0.0	0.0	0.0	100	100
P wave velocity	m/sec	0.0	0.0	0.0	1000	1000
Transformation stress ratio (M_m)		0.909	0.909	0.817	0.909	0.909
Fracture stress ratio (M_f)		1.229	1.229	1.245	1.229	1.229
Prameter in hardeining function (B_0)		3500	3500	5186	2000	2000
Prameter in hardeining function (B_1)		0.0	60	100	40	40
Prameter in hardeining function (C_f)		0.0	0.0	0.0	0	0
Anistropic loss parameter (C_d)		2000	2000	2000	2000	2000
Plasticity reference strain (γP^*r)		1000	0.003	0.005	1000	0.005
Elastic reference strain (γE^*r)		1000	0.006	0.02	1000	0.003

Table 4. Structural property value.

			Unit	Iron plate	Steel sheet pile	Wire	Tie rod
Elastic modulus			kN/m^2	205000000	210000000	205000000	210000000
Unit volume weight			kN/m^2	76.44	73.6	76.44	73.6
Rigidity		Area	m^2	0.392	0.0153	0.001256	0.00159
		Second moment of area	m^4	0.000052267	0.0000874	1.0E-11	1.0E-11
		Effective shear area ratio		0.833			
		Section modulus	m^3	0.00261333	0.00087400	—	—
		Plastic section modulus	m^3	0.00392			
non-linear Consideration	Yield stress		kN/m^2	175000	295000	—	—
	Bending moment	Mf1	kN*m	457.33275	802		
		Mf2	kN*m	686	1.0E+08		
	Reduction factor	a1		0.01	0.01	—	—
		a2		1	1		
		a3		1	1		

4 LIQUEFACTION EXPERIMENT BY DYNAMIC CENTRIFUGE

4.1 *Condition of experiment*

The liquefaction experiment was performed using the centrifuge model test equipment by Kochi National College of Technology. In this study, the centrifugal force field was set to 40G. Therefore, the model size used was 1/40 of the actual size. Table 6 shows the experimental conditions (Japan Road Association 2012). Figure 12 shows the input seismic wave in the experiment.

Table 5. Analysis condition.

Static analysis data	
Constitutive model	elastic perfectly plastic model
Mesh set	embankment ･liquefaction layer ･base layer
Boundary set	displacement fixed ･drainage boundary
Weight set	Self Weight
Ground acceleration	none
analysis/output control data	
Calculation time increment (s)	0.01
Output time increment (s)	0.1
Time integration method	Newmarkβ method (coefficient:β=0.3025 γ=0.6)
Rayleigh damping	Mass proportional=0 Stiffness proportional=0

Dynamic analysis data	
Constitutive model	cyclic elasto-plasticity model
Mesh set	embankment ･liquefaction layer ･base layer
Boundary set	displacement fixed ･drainage boundary ･attribute change
Weight set	none
Ground acceleration	Input seismic wave
analysis/output control data	
Calculation time increment (s)	0.001
Output time increment (s)	0.1
Time integration method	Newmarkβ method (coefficient:β=0.3025 γ=0.6)
Rayleigh damping	Mass proportional=0 Stiffness proportional=-0.003

Table 6. Experimental condition.

Experimental tank	Rigid earthen tank (W:450mm, H:365mm, D:140mm)
Centrifuge force field	40G
Base layer	Toyoura standard sand, Dr =70%, (Air fall method)
Liquefaction layer	Toyoura standard sand, Dr=50 % (Water fall method)
Input seismic wave	sin wave, period 20s, displacement 3mm, frequency 20Hz
Measurement items	Acceleration of in-ground and quay Pore water pressure in the ground Settlement process and cross-sectional displacement process of back ground of sheet pile

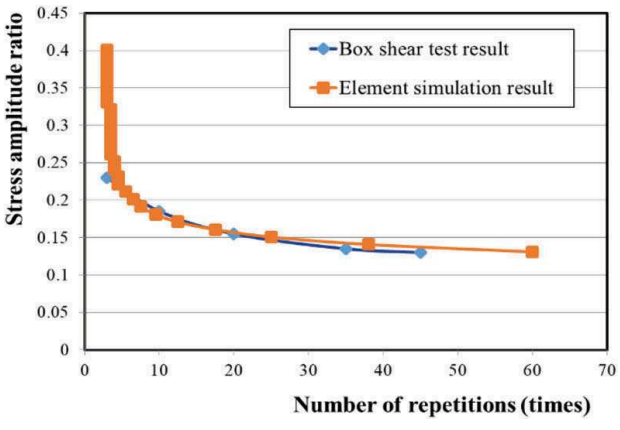

Figure 11. Elemental simulation (liquefaction resistance).

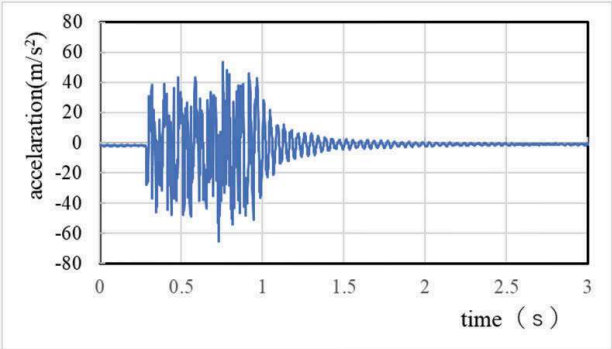

Figure 12 . Input seismic wave.

Figure 13. Experimental soil layer (Case1 before vibration).

4.2 *Experiment method*

The experimental soil layer is made using Toyoura sand. Base layer Dr = 70%, the liquefiable layer is in Dr = 50%. The sandbags used in Case3 and Case4 were created by putting light gravel material (pearl white: γ_t = 16.02kN/m^2) in a highly permeable bag (non-woven), and stacking it on the back of the quay.

Also, a viscous liquid with viscosity 40 times that of water is used according to the similarity law by mixing water and methylcellulose.

The completed experimental soil layer is placed on the shaking table of the centrifuge model test equipment and the experiment was performed. The centrifugal force up to 40G is applied and the input wave is loaded by the shaking table. After the experiment was completed, the position of the target in the soil layer and the deformation of steel sheet pile was measured. Also measured the deformation of steel sheet pile. Figure 13 shows the completed experimental soil layer (Case1).

5 RESULT AND DISCUSSION

Figure 14 shows the extraction position of the final deformation value and of the time history of the excess pore water pressure ratio. The deformation values at the specific nodes and the excess pore water pressure ratio in the specific elements as indicated in Figure 7 are shown in the next paragraph.

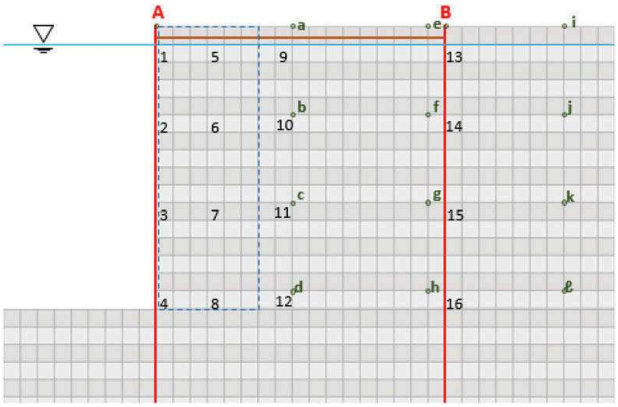

Figure 14. Result extraction point.

5.1 *Analysis result*

5.1.1 *Deformation and settlement*

Table 7 shows the final deformation of analysis results. From Table 7, the horizontal displacement is the largest in Case1 (1.57m at the top of the sheet pile) where no countermeasures have been taken, and smaller in Cases2 to 4(0.88m at the top of the sheet pile). In addition, Case3 and Case4 are smaller than Case2 on the back surface of the sandbag (0.46m at point c, about 0.33m at point d). Case1 has the largest backfill on the back of the wall (1.55m at point a), and Cases2 to 4 have the largest backfill on the back of the counterfort (about 1.06m at point i).

5.1.2 *Excess pore water pressure ratio*

Figure 15 shows the time history of the excess pore water pressure ratio of elements 6 to 8. The excess pore water pressure ratio in Case1 and Case2 reached 1.0 and were completely liquefied. The excess pore water pressure ratios of Case3 and Case4 were small, and it can be seen that the liquefaction countermeasure effect was achieved by increasing the drainage property due to the gravel in the sandbag.

5.1.3 *Comparison of each case*

Figure 16 shows the final deformation after vibration and the excess pore water pressure ratio distribution,

Table 7. Final deformation (analysis results).

Vertical displacement	a	b	c	d	e	f	g	h	i	j	k	l	Maximum settlement	Maximum uplift
Case1	-1.552	-0.914	-0.484	-0.191	-1.102	-0.780	-0.505	-0.298	-0.670	-0.529	-0.382	-0.254	-1.697	
Case2	-0.340	-0.230	-0.182	-0.139	-0.936	-0.949	-0.765	-0.402	-1.067	-0.610	-0.327	-0.103	-1.069	0.160
Case3	-0.143	-0.099	-0.073	-0.115	-0.511	-0.650	-0.684	-0.399	-1.050	-0.603	-0.322	-0.097	-1.071	0.116
Case4	-0.137	-0.100	-0.076	-0.116	-0.603	-0.696	-0.696	-0.402	-1.060	-0.617	-0.328	-0.100	-1.071	0.121
Horizontal displacement	a	b	c	d	e	f	g	h	i	j	k	l	A	B
Case1	0.032	-0.297	-0.404	-0.328	0.665	0.397	0.101	-0.014	0.894	0.734	0.410	0.194	-1.567	
Case2	-0.859	-0.786	-0.768	-0.466	-0.836	-0.694	-0.543	-0.373	0.331	0.054	-0.177	-0.228	-0.888	-0.901
Case3	-0.926	-0.432	-0.459	-0.330	-0.801	-0.636	-0.509	-0.363	0.337	0.034	-0.206	-0.240	-0.889	-0.903
Case4	-0.923	-0.454	-0.476	-0.336	-0.772	-0.648	-0.510	-0.364	0.353	0.046	-0.201	-0.238	-0.887	-0.901

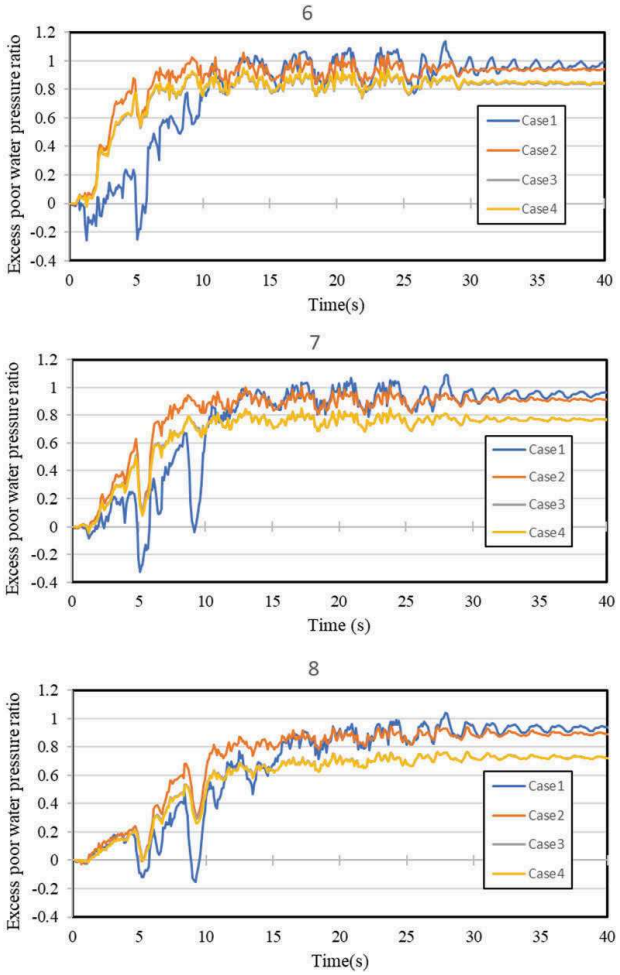

Figure 15. Time history of excess pore water pressure ratio.

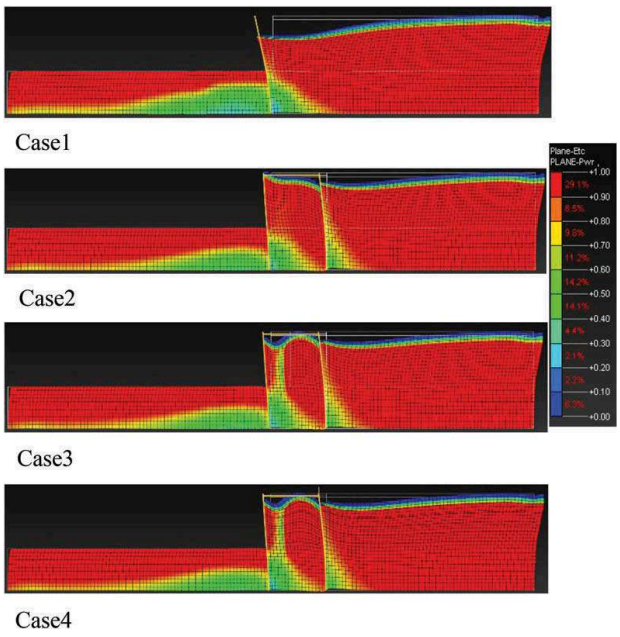

Figure 16. Displacement and excess pore water pressure ratio.

respectively. The excess pore pressure ratio increases as the element changes from blue to red. The red color shows where the excess pore water pressure is 1.0. It indicates that complete liquefaction has occurred.

In Case1, large settlement and lateral flow were observed at the back of the sheet pile. Case2 has lower horizontal and vertical displacements overall than Case1. However, the excess pore water pressure ratio at the back of the sheet pile is increasing.

The maximum settlement of the sandbag in Case3 was 1.071 m. This is due to the unit weight of the sandbag being larger than the Toyoura standard sand, which caused the settlement. There was almost no change in horizontal displacement. The excess pore pressure ratio decreased in the sandbag compared to Case2. In Case4, both the displacement and the excess pore water pressure ratio were not much different from Case3. The excess pore water pressure ratio on the ground surface was smaller than in Case3. But the change was very small.

Figure 17 shows the distribution diagrams of the horizontal stress due to the deformation of Case2 and Case4.

Each figure shows the horizontal stress at 24.4s. The maximum value of the element is 510.93 (kN/m²) for Case2, 560.91 (kN/m²) for Case4, which is larger in Case4 than in Case2. The unit weight of the sandbag is larger than that of Toyoura standard sand, so it is considered that the horizontal stress acting on the steel sheet pile when lateral flow occurred was increased.

5.2 *Experiment result*

Figure 18 shows the experimental soil layer after vibration. Table 8 shows the displacement at each point, and Figure 19 shows the time history of excess pore water pressure ratio.

5.2.1 *Horizontal displacement and settlement*

From the Table 8, the destruction occurred in Case1, and the horizontal displacement of the back surface

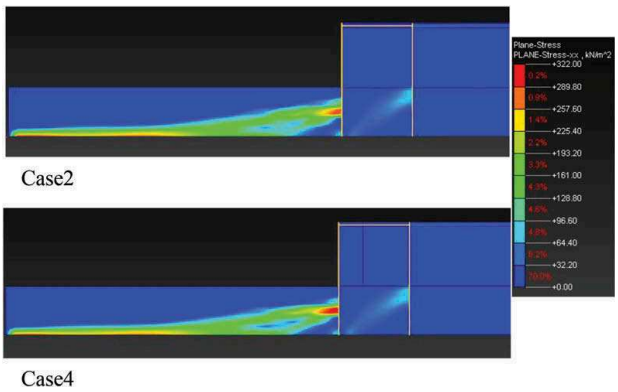

Figure 17. Horizontal stress distribution.

Case1

Case2

Case3

Case4

Figure 18. Experimental result.

of the sandbag was large at all points a to d (Point a is unmeasurable, point b is 1.44 m, point c is 0.92 m). The settlement showed the same tendency as the horizontal displacement.

Vertical displacement	a	b	c	d	e	f	g	h	i	j	k	ℓ
Case1		0.720	0.920	0.160		0.880	0.360	0.080		0.080	0.000	0.000
Case2	0.920	0.080	0.000	0.000	0.920	0.040	0.000	0.000	0.720	0.520	0.200	0.000
Case3	0.280	0.600	0.360	0.080	0.480	0.360	0.240	0.120	0.000	0.480	0.400	0.000
Case4	0.280	0.160	0.000	0.000	0.040	0.120	0.200	0.000	0.520	0.080	0.000	0.000
Horizontal displacement	a	b	c	d	e	f	g	h	i	j	k	ℓ
Case1		1.440	0.920	0.160		0.880	0.360	0.080		0.080	0.000	0.000
Case2	0.800	0.200	0.120	0.080	0.000	0.080	0.040	0.040	0.000	0.000	0.200	0.000
Case3	0.440	0.360	0.400	0.000	0.280	0.240	0.200	0.120	0.000	0.000	0.000	0.000
Case4	0.120	0.000	0.000	0.080	0.040	0.000	0.200	0.000	0.120	0.000	0.000	0.000

Table 8. Final deformation (experimental results)

5.2.2 *Excess pore water pressure ratio*

From the Figure 19, at the upper part (10, 11) of Case1, complete liquefaction occurred, and settlement and lateral flow at the back of the sheet pile were confirmed. The reason why the pore water pressure ratio exceeds 1.0 at the upper part was considered to be that the pore water pressure gauge sank due to liquefaction and the excess pore water pressure increased.

In Case2, the deformation was suppressed (0.80m at point a), and the excess pore water pressure ratio was also reduced compared to Case1.

In Case 3, the excess pore water pressure ratio was larger in the upper part of the back of the sandbag than in Cace 2. It is considered that this is because the deformation was suppressed (0.44m at point a, 0.36m at point b and 0.40m at point c) and the volume of the void became smaller than that of Case 2.

In Case4, the deformation of the experimental soil layer became very small (0.12m at point a, 0m at points C to d). The excess pore water pressure ratio also became the smallest. This is because the pore water was drained by the permeable steel sheet pile. Therefore, it can be seen that by using the sandbag and the permeable steel sheet pile, the drainage property of the backfill soil and the sheet pile was improved, and the liquefaction countermeasure effect was improved.

6 COMPARISON BETWEEN ANALYSIS RESULT AND EXPERIMENTAL RESULT

Table 9 shows the displacement of the analysis results for the experimental model, and Figure 20 shows a comparison diagram. The analysis results and experimental results were compared for Case1, Case2, and Case4. In Case3, the liquefaction countermeasure effect was not so different from Case2, so it is omitted here.

From the comparison between Case1 and Case2, the deformation was almost the same.

In Case4, the experimental deformation was smaller than the analytical deformation. The reasons for this are as follows: (1) In the experiment, the drainage effect of sandbags and permeable steel sheet

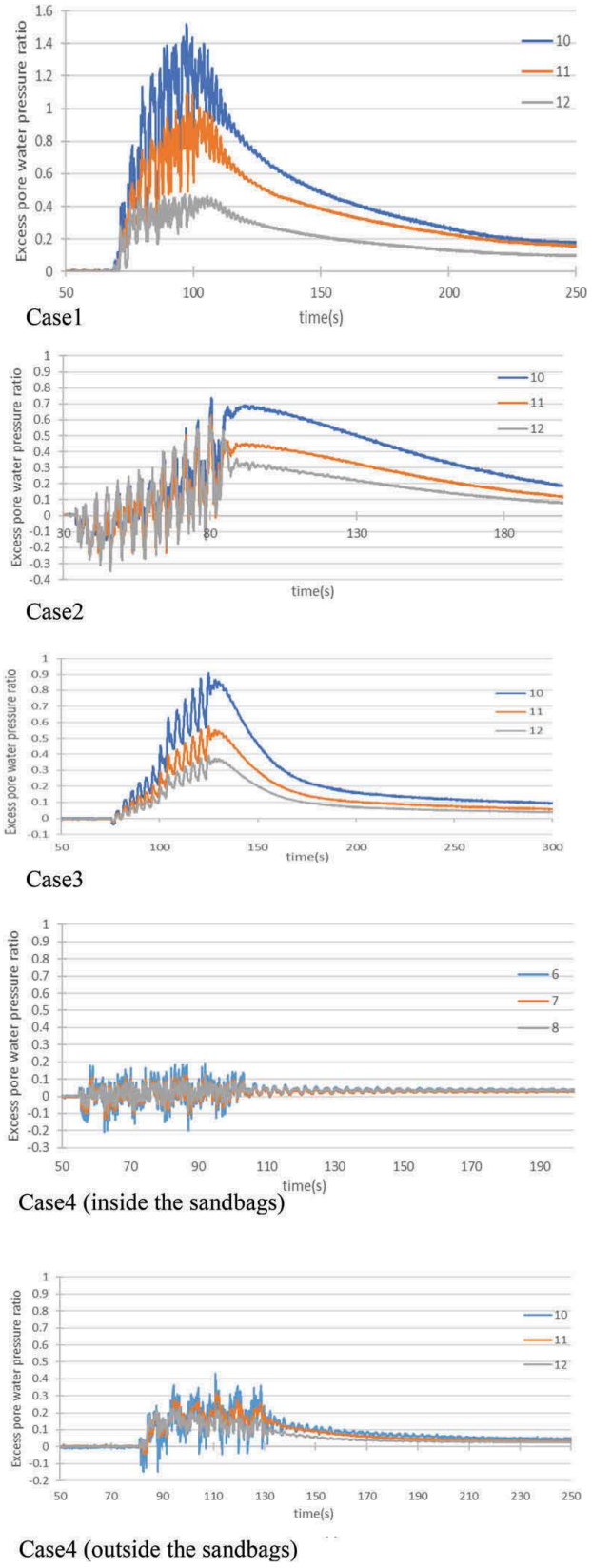

Figure 19. Experimental results.
(Time history of excess pore water pressure ratio)

piles was high, and the pore water was dissipated and the liquefaction was suppressed. (2) In the experiment, the deformation of the backfill soil was suppressed by the integration effect of the sandbags, but it could not be considered in the analysis. (3) In the analysis, the permeability of sandbags and permeable sheet piles was evaluated to be smaller than that of the experimental model.

Vertical displacement	a	b	c	d	e	f	g	h	i	j	k	ℓ
Case1	-0.897	-0.559	-0.294	-0.126	-0.560	-0.380	-0.217	-0.101	-0.249	-0.083	-0.051	-0.036
Case2	-0.089	0.011	0.029	0.002	-0.621	-0.621	-0.483	-0.158	-0.677	-0.525	-0.370	-0.177
Case3	0.041	0.090	0.101	0.004	-0.269	-0.354	-0.439	-0.203	-0.610	-0.471	-0.330	-0.157
Case4	0.209	0.138	0.110	0.016	-0.245	-0.262	-0.400	-0.198	-0.606	-0.471	-0.330	-0.156
Horizontal displacement	a	b	c	d	e	f	g	h	i	j	k	ℓ
Case1	-0.780	-0.556	-0.373	-0.195	-0.612	-0.170	-0.063	-0.036	-0.513	0.009	0.075	0.033
Case2	-0.887	-0.723	-0.626	-0.374	-0.831	-0.672	-0.500	-0.327	-0.471	-0.176	-0.275	-0.223
Case3	-0.946	-0.369	-0.300	-0.198	-0.766	-0.577	-0.422	-0.272	-0.440	-0.137	-0.250	-0.206
Case4	-1.184	-0.318	-0.238	-0.173	-0.937	-0.570	-0.412	-0.270	-0.432	-0.134	-0.250	-0.206

Table 9. Final deformation (Analysis results of experimental model)

7 CONCLUSION

In this study, we investigated the liquefaction countermeasures for fishing port quays using double steel sheet piles, sandbags and permeable steel sheet piles. The following conclusion were obtained.

(1) The sandbag had the effect of dissipating the pore water pressure inside the sandbag, and the permeable steel sheet pile had the effect of draining the pore water on the back of the quay. It was confirmed that the effect of liquefaction countermeasures on the quay was improved by using both.
(2) The uncountermeasured model and the double sheet pile model of the centrifuge experiment could be reproduced because the displacement and subsidence were almost the same as the seismic response analysis simulation using LIQCA (2015).
(3) In the actual model with a larger analysis boundary, the amount of settlement was smaller than that of the experimental model, but the horizontal displacement was about the same.
(4) In the Case of the model equipped with sandbags and permeable sheet piles, the centrifugal experiment showed more dissipation of excess pore water pressure than the LIQCA analysis, and the effect of liquefaction countermeasures was higher. The reason may be that the water permeability was evaluated to be smaller than that of the experimental model in the analysis, and the integration effect of sandbags could not be considered.

REFERENCES

Japanese Association for Steel Pipe Piles, 2017. *Steel sheet pile Q&A*: 33–38

Japan Road Association, 2012. *Specifications for highway briges PartV seismic design. (in Japanese)*

LIQCA Liquefaction Geo-Research Institute, 2015. *LIQC A2D15· LIQCA3D15(2015) release version document Part1 Theory*: 1–55

NIPPON STEEL CORPORATION, 2019. *Steel sheet pile, catalog.*7. https://www.nipponsteel.com/product/catalog_download/pdf/K007.pdf

Saito, K. 2016. Simulation analysis of centrifuge model experiment using liquefaction analysis program LIQCA: 14

Tanimoto, W., Okabayashi, K., Mukaidani, M., and Hama, K. 2019. Reiwa 1st Japan Society of Civil Engineers National Convention 74th Annual Scientific Lecture (III-311). *Comparison of Kochi College type cyclic box shear apparatus with cyclic triaxial apparatus*.

Tokuhisa, K. 2016. Thesis Research Reports, ADVANCE COURSE KOCHI NATIONAL COLLEGE OF TECHNOLOGY, 15th. *A study on the liquefaction countermeasures of wharf considering the Nankai Trough earthquake*: 12